Sub-harmonic injection locking of quantum-dash lasers using spectral enrichment from semiconductor optical amplifiers

MANAS SRIVASTAVA,[1],* PRINCE ANANDARAJAH,[2] BALAJI SRINIVASAN,[1] SEAN O'DUILL,[2] DEEPA VENKITESH,[1] AND PASCAL LANDAIS[2]

[1]Department of Electrical Engineering, Indian Institute of Technology Madras, Adyar, Chennai 600036, India
[2]The Radio and Optics Research Laboratory, School of Electronic Engineering, Dublin City University, Glasnevin, Dublin 9, Ireland *Corresponding author: ee13d057@ee.iitm.ac.in

We report sub-harmonic injection locking of a 40 GHz passively mode-locked quantum-dash (Q-dash) laser through spectral enrichment in a nonlinear semiconductor optical amplifier. The proposed scheme demonstrated for injection locking of the Q-dash passively mode-locked laser using data modulated with non-return-to-zero line-coding at 10 G symbols/s with both intensity and phase shift keying modulations.

1. INTRODUCTION

Passively mode-locked quantum-dash (Q-dash) lasers have attracted much attention for several applications, such as super continuum generation [1], millimeter-wave upconversion [2], and gas sensing [3], due to their excellent phase noise and timing jitter characteristics [4–7]. In addition, the superior injection-locking performance [8] is found to be quite useful for applications including sub-picosecond pulse generation [9], optical frequency comb generation [10], and all-optical clock recovery [11]. In particular, clock recovery through injection locking has been demonstrated for 40 Gbps [12] and its harmonics up to 320 Gbps [13,14] as they are resonant with the fundamental round-trip frequency of 40 GHz in the Q-dash structures [4]. However, the 40 GHz Q-dash platform is not amenable to recovering the clock from the 10 Gbps data stream in existing telecom systems. As such, a spectral enrichment of the above data stream is critical for the injection locking of the Q-dash laser.

The above-mentioned need for spectral enrichment is particularly critical in the case of 10 Gbps non-return-to-zero on– off keying (NRZ-OOK) and binary phase shift keying (BPSK) modulation as they have a weak component at 40 Gbps owing to the limited bandwidth of the corresponding transmitters. This spectral enrichment is typically carried out by passing the signal through optical nonlinear media to facilitate the mixing of the spectral components of the signal, thus enhancing the power in the clock tones. Highly nonlinear fibers, photonic crystal fibers, silicon waveguides, and semiconductor optical amplifiers (SOA) [15] have been used in the past for spectral enrichment. Compared to the above-mentioned approaches, spectral enrichment using SOAs is preferred due to their superior conversion efficiencies and compact footprint. They have been successfully used in several applications that require high nonlinear conversion efficiencies such as wavelength conversion [16], phase conjugation [17], and format conversion [18].

SOAs have also proved to be efficient in time-domain and spectral-domain shaping of signals and selective enhancement and/or suppression of spectral components. Specifically, for timing-related applications, they have been used to enhance the clock tones, leading to clock-to-data suppression in the sig-nal spectrum [19]. The nonlinear distortion of the signal wave-form in an SOA may be efficiently utilized in converting an NRZ signal to a pseudo-return-to-zero (PRZ) waveform, which has stronger clock tones in the spectrum compared to the original NRZ signal. An NRZ-to-PRZ conversion stage based on SOA has been demonstrated for fundamental injection locking with 40 Gbps NRZ data [20].

In this paper, we demonstrate sub-harmonic injection lock-ing of a Q-dash laser at 40 GHz through spectral enrichment of 10 Gbps NRZ data. Such an injection-locking technique may be extended to higher-order modulation formats such as quartenary pulse amplitude modulation (4-PAM) and differential quadrature phase shift keying (DQPSK), which still use direct detection receivers where electronic clock recovery is increasingly challenging at higher baud rates. Moreover, optical clock recovery with M-ary quadrature amplitude modulation (m-QAM) formats could prove useful for all-optical sampling ap-plications [21].

This paper is organized in the following manner. The free-running characteristics of the Q-dash laser used in the experiments are described in Section 2. Section 3 provides the details on the spectral enrichment of band-limited NRZ signals and the corresponding experimental results. Experiments on injection locking using spectrally enriched signals and subsequent conditioning of the injection-locked signal are discussed in Section 4. Finally, the conclusions are presented in Section 5.

2. FREE-RUNNING CHARACTERISTICS OF A Q-DASH LASER

The Q-dash laser is initially characterized in a passively mode-locked condition without any signal injection (free-running condition). A basic L–I characterization reveals that the lasing threshold of the Q-dash laser is ~16 mA. Figure 1 shows the output of the Q-dash laser in the free-running condition (operating current of 180 mA, optical power of 4.8 dBm) measured using a photodetector (u2t XPDV2120R; bandwidth ~50 GHz) on an electrical spectrum analyzer (ESA; Anritsu 2668C; bandwidth 40 GHz). The peak of the beat spectrum is observed at ~39.8 GHz as shown in Fig. 1. The radio frequency (RF) spectrum is found to be shifting with time, mainly due to environmental fluctuations, and the maximum shift in the peak of the spectrum was recorded to be <200 kHz for a time of observation of more than 1 min.

The inset of Fig. 1 shows the optical spectrum of the Q-dash laser in the free-running condition measured using the optical spectrum analyzer (OSA, Anritsu MS9710B; resolution 0.05 nm) A comb of spectral lines with a spacing of ~0.32 nm, corresponding to a longitudinal mode of the laser with a frequency separation of ~39.8 GHz is observed on the OSA. The number of mode-locked components increases with the drive current. At sufficiently high currents (>150 mA), as many as 40 longitudinal modes of the Q-dash laser are seen to be locked. Power differences between these modes are found to be within 3 dB with a carrier-to-noise ratio (CNR), exceeding 30 dB over a wavelength range of 1518–1532 nm [22]. However, there is a definite possibility of achieving injection locking with the carrier wavelength of the injected signal at larger wavelengths in the C-band since the Q-dash laser is expected to be transparent at longer wavelengths.

3. SPECTRAL ENRICHMENT OF NRZ SIGNALS

In order to achieve injection locking at 40 GHz from a 10 Gbps signal, the injected signal must have spectral components at 40 GHz. This is achieved by passing the signal through a non-linear medium and generating the required harmonics through four-wave mixing. Hence, the signal is passed through a non-linear SOA (CIP SOA-XN-OEC-1550), where it undergoes spectral enrichment due to gain saturation and consequent generation of intermodulation products, leading to four-wave mixing in the SOA [23]. The generated 40 GHz sidebands make the signal suitable for injection locking.

Figure 2 shows the experimental setup used for spectral enrichment. A tunable laser source (TLS; Agilent N7711A) is used to provide the optical carrier. The carrier wavelength and power are set as 1535 nm and 6.5 dBm, respectively. A Mach–Zehnder modulator (MZM) is used to modulate the carrier. The modulating signal is a $2^7 - 1$ long pseudo-random bit sequence (PRBS) at a bit rate of 10 Gbps, provided by a pulse pattern generator (PPG; Anritsu MP1800A). The bias voltage for the MZM is set to the quadrature point, and the

polarization of the laser is adjusted to ensure the maximum extinction ratio required to get the best eye pattern for the NRZ-OOK signal. An Erbium-doped fiber amplifier (EDFA) is used to boost the power at the output of the modulator to ~9 dBm such that it saturates the SOA.

Figure 3 shows the optical spectra of the original OOK signal and the signal after spectral enrichment for SOA bias currents of 200 mA and 400 mA, measured using a high-resolution OSA (Apex AP 2043B) with a resolution bandwidth of 0.16 pm. The 10 GHz and 20 GHz sidebands in the original signal are seen to be ~−30 dBc and ~−50 dBc, respectively. After enrichment, they are found to be ~−20 dBc and ~−30 dBc, respectively, and additional sidebands with separa-tion ≥30 GHz from the carrier wavelength are also generated [24]. The asymmetric nature of the enriched spectrum is well-studied and is attributed to the interplay between the various nonlinear mechanisms in the SOA [25,26].

Figure 4(a) shows the overlaid portions of the RF spectrum of the NRZ-OOK signal at the input of the SOA, where strong components are present at 10 GHz and 20 GHz, whereas the 30 GHz and 40 GHz components are completely absent. These components appear only after passing the modulated signal through the SOA, as shown in Fig. 4(b). Due to enrichment of the optical spectrum, several new components are generated that result in the generation of RF beat components at 30 and 40 GHz. It should also be noted that the power in the 40 GHz tone is ~30 dB smaller than that in the 10 GHz tone.

The experiment discussed above is also extended to BPSK signals. In order to generate an NRZ-BPSK waveform, the bias of the MZM is adjusted to its null point, and the modulation signal is applied. The BPSK signal is subjected to spectral enrichment in a manner similar to the NRZ-OOK signal. Subsequently, the spectra and waveform of the signal before and after enrichment are observed. Spectral broadening is observed for the NRZ-BPSK signal as well, but the enriched signal is found to be broadened on both sides as opposed to the case of the NRZ-OOK signal as seen in Fig. 5. In the NRZ-OOK signal, there are well-defined clock tones that gain power and become enhanced as a result of spectral enrichment. On the other hand, there are no discrete clock peaks in the spectrum of the original NRZ-BPSK signal. Hence, after spectral enrichment, the power is distributed over a larger spectral width, leading to a broader spectrum compared to the case of NRZ-OOK signals. A comparison of the RF spectra of the original and the enriched signal is given in Fig. 6 and reveals that the 30 GHz and 40 GHz are generated with significant power, once again indicating the suitability of this signal for injection locking.

The frequency content of the signal that undergoes enrichment is dependent on the length of the pseudo-random sequence used. The effect of the length of the random bit sequence is analyzed through numerical simulations. The propagation model of SOAs [27,28] is used to study the spectral enrichment process of OOK and BPSK signals of the lengths of the random bit signal varying from 27 − 1 to 231 − 1. The carrier-to-sideband power ratio (CSR) for the 10 GHz sidebands of the signals before and after propagation through the SOA is measured, and its variation with respect to the PRBS order is observed. The extent of spectral enrichment is characterized by the change in the CSR before and after the propagation through the SOA. The results are shown in Fig. 7. In case of the NRZ-OOK signal, the change in CSR is >35 dB for all values of PRBS order. The slight difference in the extent of enrichment of the 10 GHz and −10 GHz sidebands is indicative of the asymmetry in the four-wave mixing process in the SOA and is consistent with the experimental results reported above.

The change in CSR for NRZ-BPSK signals is found to be ~10–15 dB with a pronounced asymmetry in the enrichment, as shown in Fig. 7 (right). The nonuniformity in the CSR originates due to the variation in the spectral content of the signal with respect to PRBS order. Longer PRBS orders cause lower frequency components to be generated in the signal spectrum. The performance of spectral enrichment is better in such cases due to improved gain reduction at lower frequencies, owing to the high-pass nature of the gain characteristics of the SOA [29]. Even though the experiments were performed with a PRBS order of $2^7 − 1$, we conclude from these numerical simulations that the quality of injection locking—which is in turn dependent on the strength of the enriched tones—is independent of the PRBS order, and hence the SOA-based spectral enrichment is suitable for any practical data stream.

4. INJECTION LOCKING

The enriched signal can be used to injection lock the Q-dash laser if the spectral components are coincident with the modes of the FP cavity of the laser. The carrier wavelength of the data signal is suitably chosen to ensure the same. Thereafter, the data rate is varied to measure the range of injection locking.

A. Injection Locking with NRZ-OOK Data

Figure 8 shows the experimental setup for injection locking of a Q-dash laser using the enriched NRZ-OOK signal. The carrier wavelength is tuned from 1534.52 to 1535.52 nm in steps of 0.04 nm (~5 GHz), keeping the data rate fixed at 9.9515 Gbps in order to investigate the injection-locking phenomenon. Figure 9(a) shows the RF beat spectrum of the output of the Q-dash laser for different values of carrier wavelength. As we tune the carrier wavelength, we observe a corresponding shift in the free-running peak in the RF spectrum of the Q-dash laser without any noticeable change in the spectral quality of the peak. However, an additional peak appears at 39.806 GHz when the carrier wavelength is 1535.08 nm and 1535.40 nm, as shown in bold lines in Fig. 9(a). Upon further investigation, we find that the additional peak corresponds to the fourth harmonic of the modulated data rate, which indicates the possibility of injection locking. In order to confirm this, we measure the power at 39.806 GHz as a function of carrier wavelength. As shown in Fig. 9(b), the power measured at 39.806 GHz is maximum for carrier wavelengths separated by 0.32 nm (40 GHz). Since this separation corresponds to the longitudinal mode spacing of the Q-dash laser, we can deduce that injection locking is achieved when the spectral components of the injected signal are coincident with the longitudinal modes of the Q-dash laser. Thus, injection locking could be achieved if the carrier wavelength is tuned to one of these suitable values. In a practical scenario, the spectrum of the Q-dash laser can be tuned by varying the driving current or the temperature in order to match the carrier wavelength. Based on the observations detailed above, the carrier wavelength is chosen to be 1535.40 nm. Optical power injected in the Q-dash laser is ~10 dBm. In order to estimate the range of locking frequencies, the modulation data rate is varied from 9.948 to 9.95 Gbps in steps of 100 kbps.

The RF beat spectra of the Q-dash laser in free-running and various conditions of injection are shown in Fig. 10. It is seen that the injection of a continuous wave (CW) laser shifts the free-running frequency of the Q-dash laser by 1.7 MHz. This could be attributed to the change in the refractive index, and consequently the effective round-trip frequency of the Q-dash laser under CW injection. The width of the RF beat tone (referred to as RF linewidth) is seen to increase from ~105 kHz to ~175 kHz. All the RF linewidths are estimated by fitting the experimentally recorded spectrum to a Lorentzian profile. Injection of spectrally enriched NRZ-OOK data results in the locking of Q-dash laser modes to the fourth harmonic of the injected signal. This is evident in the RF spectrum (Fig. 10 bottom), as the beat tone of Q-dash laser modes appears exactly at 4 times the frequency of the data rate. The linewidth of the beat tone is reduced to <30 kHz upon injection, indicating efficient injection locking. As the data rate is tuned, the beat tone also shifts, as seen in Fig. 10. Injection locking is achieved for the range of modulation data rates 9.9482–9.9495 Gbps, which corresponds to a locking range of 4 × 9.9495 − 9.9482 GHz 5.2 MHz [24].

The optical spectrum of the Q-dash laser output around the injected signal, as shown in Fig. 11(a), reveals the positions of the carrier wavelength and sidebands with respect to the free-running modes of the Q-dash laser in the injection-locked con-dition. It can be observed that the chosen carrier wavelength (1535.40 nm) is such that the 10 GHz sideband coincides with one of the modes of Q-dash laser. Due to injection locking, modes of the Q-dash laser also become enhanced.

One particular mode of the Q-dash laser is observed minutely in the free-running and the injection-locked conditions, as shown in Fig. 11(b). The mode is found to shift from its free-running position by ~0.11 nm after

injection. Optical linewidth measured at 20 dB of the mode has reduced from ~138 MHz in the free-running condition to ~90 MHz in the injection-locked condition.

It is also independently verified that injecting a signal amplified to ~10 dBm through an EDFA (instead of an SOA) does not result in locking of the Q-dash laser, since the EDFA does not selectively enhance the power of the higher-frequency spectral components. It is the nonlinear mixing in the SOA that causes the higher harmonics to get enhanced, thus facilitating injection locking.

B. Injection Locking with NRZ-BPSK Data

We now present the results of injection locking for spectrally enriched NRZ-BPSK data. All other experimental conditions are similar to those discussed in Section4.A. The results obtained show trends similar to those obtained in the case of the NRZ-OOK signal.
Figure 12 shows the RF beat spectrum of the Q-dash laser output in various conditions. Reduction in the beat tone line-width is seen in this case as well, with the RF linewidth observed to be<20 kHz in the injection-locked condition. Locking is achieved for modulation data rates varying from9.9497 to 9.9504 Gbps, which corresponds to a locking range of 2.8 MHz. The optical spectrum of the injection-locked output as observed around the carrier wavelength is shown in Fig.13(a). The modes of the Q-dash laser that are coincident with the sidebands of the enriched signal are found to be enhanced. One single mode of the Q-dash laser spectrum is observed in various conditions and compared as shown in Fig.13(b). The mode is seen to be shifting by~0.01 nm from its free-running position after injection. The 20 dB linewidth of the mode is seen to be reduced from~140 MHzto~115 MHz. A comparison of operating parameters and resulting locking range obtained for OOK and BPSK signals is given in Table1.

The retrieved signal is a combination of the Q-dash laser out-put after injection locking, the injected signal reflected from the Q-dash laser, as well as the crosstalk in the circulator. Hence, this signal contains features of the 10 Gbps injected signal in add it onto the injection-locked output at 40 GHz as shown in Fig.14.The output of the Q-dash laser is filtered using a bandwidth variable tunable filter (BVTF) to select a small portion of Q-dash spectrum, leaving out the residual signal. The filtered signal is amplified and the time-domain waveform is observed. The band-width of the BVTF is set to be 2.5 nm around a center wave-length of 1525 nm, thus selecting eight longitudinal modes in the central region of the Q-dash laser spectrum, as shown in Fig.15(a). The recovered 40 GHz signal as observed on the scope is shown in Fig.15(b). The recovered 40 GHz signal as observed on the scope is shown in Fig.15(b).

Since the recovered signal is observed on a sampling oscilloscope (Agilent Infiniium DCA-J 86100C) with the clock of PPG as trigger input, it may be inferred that the Q-dash laser output is synchronous with the injected NRZ signal. This signal can be further used for optical sampling [21] at a higher sampling rate with four samples per symbol, which could be beneficial for data processing in advanced modulation formats.

5. CONCLUSION

In this paper, we have demonstrated the injection locking of a 40 GHz passively mode-locked Q-dash laser with a 10 Gbps data stream modulated with NRZ-OOK and BPSK signals. Since the NRZ signals do not contain a clock tone at 40 GHz, the optical spectrum is enriched by passing the signals through a nonlinear SOA, and the required tone is generated. Data rates are selected to be the fourth sub-harmonic of the free-running frequency of the Q-dash laser. Injected power of ~10 dBm is required to achieve injection locking with the enriched data. Locking ranges of 5.2 MHz and 2.8 MHz are obtained in the case of OOK and BPSK data, respectively. The spectral enrichment technique can be ex-tended to NRZ data in higher-order modulation formats such as m-PAM and m-QAM, which have the same drawback of nonexistent or weak clock tones in the signal spectrum.

REFERENCES

1. C.-L. Tan, H. S. Djie, Y. Wang, D. N. Wang, J. C. M. Hwang, and B. S. Ooi, "Extension of quasi-supercontinuum generation in multiple-bandgap semiconductor quantum-dash laser," in Conference on Lasers and Electro-Optics/Quantum Electronics and Laser Science Conference and Photonic Applications Systems Technologies (Optical Society of America, 2008), paper CThY6.
2. M. Huchard, B. Charbonnier, P. Chanclou, F. V. Dijk, F. Lelarge, G. H. Duan, C. Gonzalez, and M. Thual, "Millimeter-wave photonic up-conversion based on a 55 GHz quantum dashed mode-locked laser," in 34th European Conference on Optical Communication (ECOC) (2008), pp. 1–2.
3. W. Zeller, M. Legge, J. Seufert, R. Werner, M. Fischer, and J. Koeth, "Widely tunable laterally coupled distributed feedback laser diodes for multispecies gas analysis based on InAs/InGaAs quantum-dash material," Appl. Opt. 48, B51–B56 (2009).
4. F. Lelarge, B. Dagens, J. Renaudier, R. Brenot, A. Accard, F. van Dijk, D. Make, O. L. Gouezigou, J.-G. Provost, F. Poingt, J. Landreau, O. Drisse, E. Derouin, B. Rousseau, F. Pommereau, and G.-H. Duan, "Recent advances on InAs/InP quantum dash based semiconductor lasers and optical amplifiers operating at 1.55 μm," IEEE J. Sel. Top. Quantum Electron. 13, 111–124 (2007).
5. J. Tourrenc, A. Akrout, K. Merghem, A. Martinez, F. Lelarge, A. Shen, G. Duan, and A. Ramdane, "Experimental investigation of the timing jitter in self-pulsating quantum-dash lasers operating at 1.55 μm," Opt. Express 16, 17706–17713 (2008).
6. R. Maldonado-Basilio, J. Parra-Cetina, S. Latkowski, and P. Landais, "Timing-jitter, optical, and mode-beating linewidths analysis on subpicosecond optical pulses generated by a quantum-dash passively mode-locked semiconductor laser," Opt. Lett. 35, 1184–1186 (2010).
7. R. Maldonado-Basilio, S. Latkowski, S. Philippe, and P. Landais, "40 GHz mode-beating with 8 Hz linewidth and 64 fs timing jitter from a synchronized mode-locked quantum-dash laser diode," Opt. Lett. 36, 3142–3144 (2011).
8. K. Merghem, S. Azouigui, A. Akrout, A. Martinez, F. Lelarge, A. Shen, G.-H. Duan, G. Aubin, and A. Ramdane, "RF linewidth narrowing in quantum-dash-based passive mode-locked lasers using optical feedback," in Conference on Lasers and Electro-Optics/International Quantum Electronics Conference (Optical Society of America, 2009), paper CTuQ3.
9. S. Latkowski, R. Maldonado-Basilio, and P. Landais, "Sub-picosecond pulse generation by 40-GHz passively mode-locked quantum-dash 1-mm-long Fabry-Pérot laser diode," Opt. Express 17, 19166–19172 (2009).
10. E. Sooudi, S. Sygletos, A. D. Ellis, G. Huyet, J. G. McInerney, F. Lelarge, K. Merghem, R. Rosales, A. Martinez, A. Ramdane, and S. P. Hegarty, "Optical frequency comb generation using dual-mode injection-locking of quantum-dash mode-locked lasers: properties and applications," IEEE J. Quantum Electron. 48, 1327–1338 (2012).
11. V. Roncin, S. Lobo, L. Bramerie, P. Rochard, A. Shen, F. V. Dijk, G. H. Duan, and J. C. Simon, "Demonstration of chromatic dispersion and optical noise insensitivity of a quantum-dash based Fabry-Perot laser in all-optical clock recovery at 40 Gbit/s," in 33rd European Conference and Exhibition of Optical Communication (2007), pp. 1–2.
12. R. Maldonado-Basilio, S. Latkowski, S. Philippe, and P. Landais, "Experimental investigation of harmonic and subharmonic synchronization of 40 GHz mode-locked quantum-dash laser diodes," Opt. Lett. 36, 1569–1571 (2011).
13. J. Parra-Cetina, S. Latkowski, R. Maldonado-Basilio, and P. Landais, "Wavelength tunability of all-optical clock-recovery based on quantum-dash mode-locked laser diode under injection of a 40-Gb/s NRZ data stream," IEEE Photon. Technol. Lett. 23, 531–533 (2011).
14. J. Cartledge, X. Tang, M. Yañez, A. Shen, A. Akrout, and G.-H. Duan, "All-optical clock recovery using a quantum-dash Fabry-Perot laser," in IEEE Topical Meeting on Microwave Photonics (MWP) (2010), pp. 201–204.
15. G. P. Agrawal, "Nonlinear fiber optics: its history and recent progress [Invited]," J. Opt. Soc. Am. B 28, A1–A10 (2011).
16. A. P. Anthur, R. Zhou, S. O'Duill, A. J. Walsh, E. Martin, D. Venkitesh, and L. P. Barry, "Polarization insensitive all-optical wavelength conversion of polarization multiplexed signals using co-polarized pumps," Opt. Express 24, 11749–11761 (2016).
17. M. Matsuura and N. Kishi, "Multichannel transmission of intensity-and phase-modulated signals by optical phase conjugation using a quantum-dot semiconductor optical amplifier," Opt. Lett. 38, 1700–1702 (2013).r

18. L. Banchi, M. Presi, A. D'Errico, G. Contestabile, and E. Ciaramella, "All-optical 10 and 40 Gbit/s RZ-to-NRZ format and wavelength con-version using semiconductor optical amplifiers," J. Lightwave Technol. 28, 32–38 (2010).

19. W. Mao, M. Al-Mumin, X. Wang, and G. Li, "All-optical enhancement of clock and clock-to-data suppression ratio of NRZ data," IEEE Photon. Technol. Lett. 13, 239–241 (2001).

20. J. Slovak, C. Bornholdt, J. Kreissl, S. Bauer, M. Biletzke, M. Schlak, and B. Sartorius, "Bit rate and wavelength transparent all-optical clock recovery scheme for NRZ-coded PRBS signals," IEEE Photon. Technol. Lett. 18, 844–846 (2006).

21. P. A. Andrekson and M. Westlund, "Nonlinear optical fiber based high resolution all-optical waveform sampling," Laser Photon. Rev. 1, 231–248 (2007).

22. R. Maldonado-Basilio, J. Parra-Cetina, S. Latkowski, N. Calabretta, and P. Landais, "Experimental investigation of the optical injection locking dynamics in single-section quantum-dash Fabry-Perot laser diode for packet-based clock recovery applications," J. Lightwave Technol. 31, 860–865 (2013).

23. A. Mecozzi, S. Scotti, A. D'Ottavi, E. Iannone, and P. Spano, "Four-wave mixing in traveling-wave semiconductor amplifiers," IEEE J. Quantum Electron. 31, 689–699 (1995).

Figures and Table
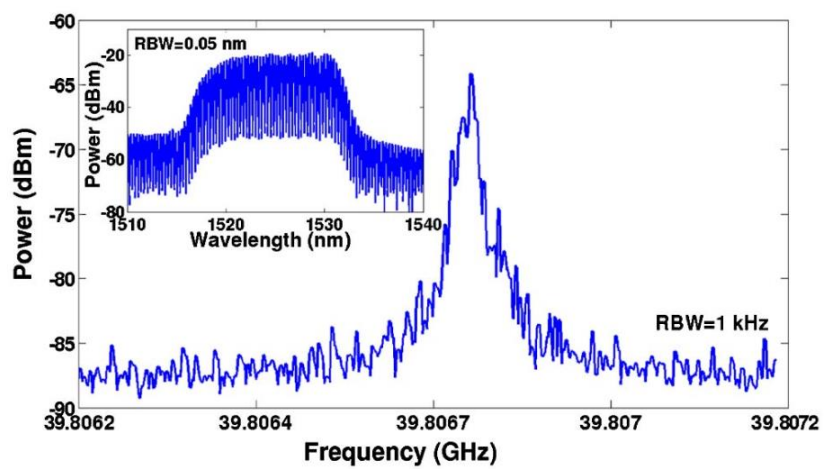
Fig. 1. RF beat spectrum of Q-dash laser output in free-running condition and the corresponding optical spectrum (inset). The peak of the RF spectrum occurs at ~39.8 GHz.
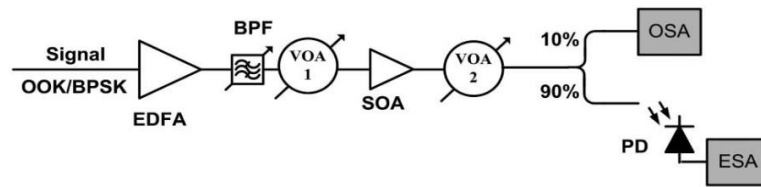
Fig. 2. Schematic for spectral enrichment of 10 Gbps PRBS bit stream. EDFA, Erbium-doped fiber amplifier; BPF, band-pass filter; VOA, variable optical attenuator; PD, photodetector.
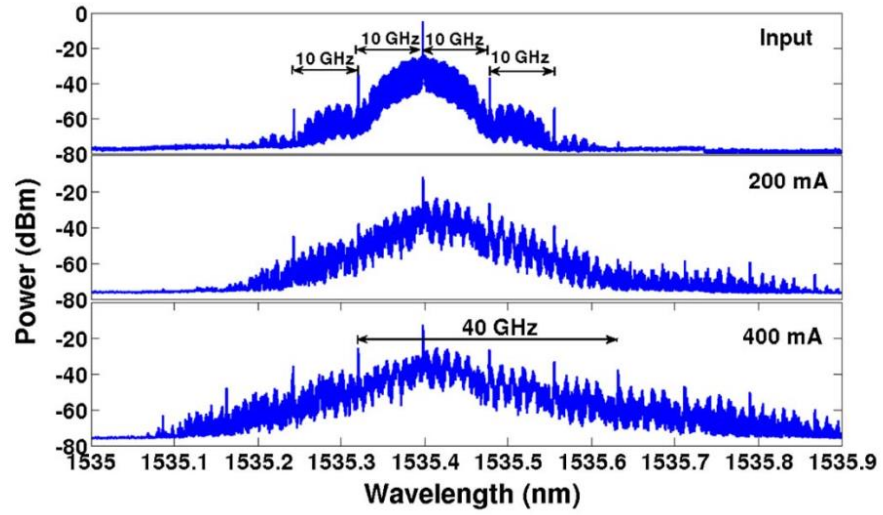
Fig. 3. Comparison of optical spectra of the 10 Gbps NRZ-OOK signal at 1535 nm and the corresponding spectrally enriched output from the SOA for various bias currents (RBW 0.16 pm).
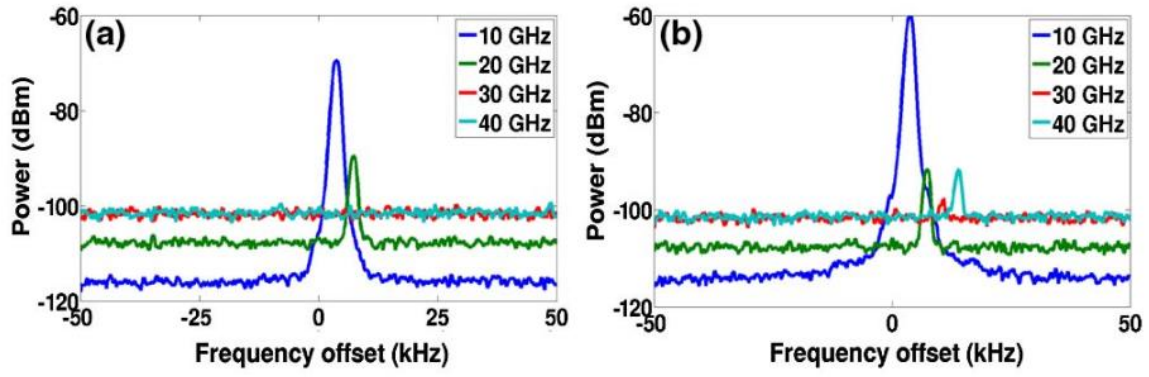
Fig. 4. Slices of the electrical RF spectrum in the vicinity of the fun-damental (10 GHz), second harmonic (20 GHz), third harmonic (30 GHz), and fourth harmonic (40 GHz) for (a) original NRZ-OOK signal and (b) spectrally enriched output of SOA with 400 mA bias current.
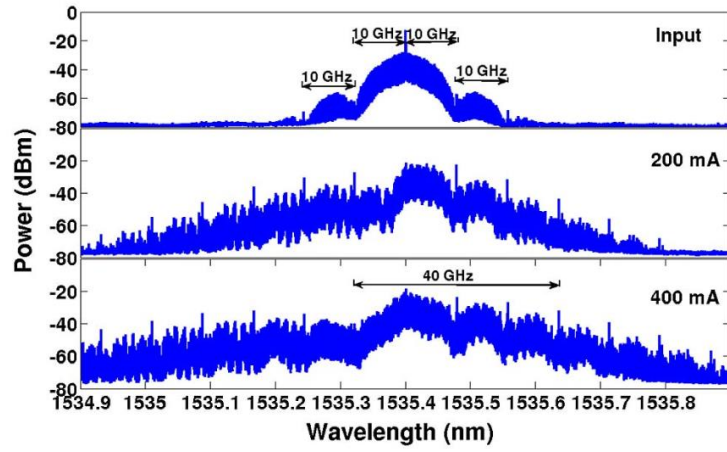
Fig. 5. Comparison of optical spectra of the 10 Gbps NRZ-BPSK signal at 1535 nm and the corresponding spectrally enriched output from the SOA for various bias currents (RBW 0.16 pm).
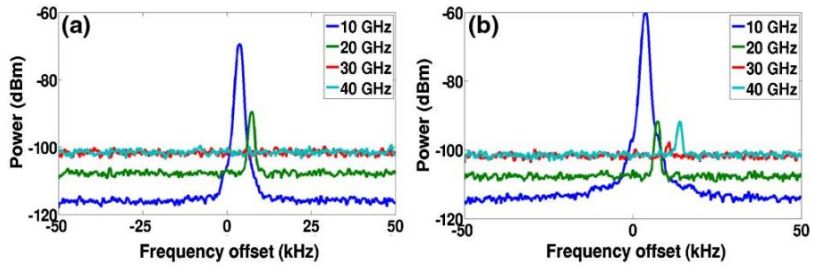
Fig. 6. Slices of the electrical RF spectrum in the vicinity of the fundamental (10 GHz), second harmonic (20 GHz), third harmonic (30 GHz), and fourth harmonic (40 GHz) for (a) original NRZ-BPSK signal and (b) spectrally enriched output of SOA with 400 mA bias current.
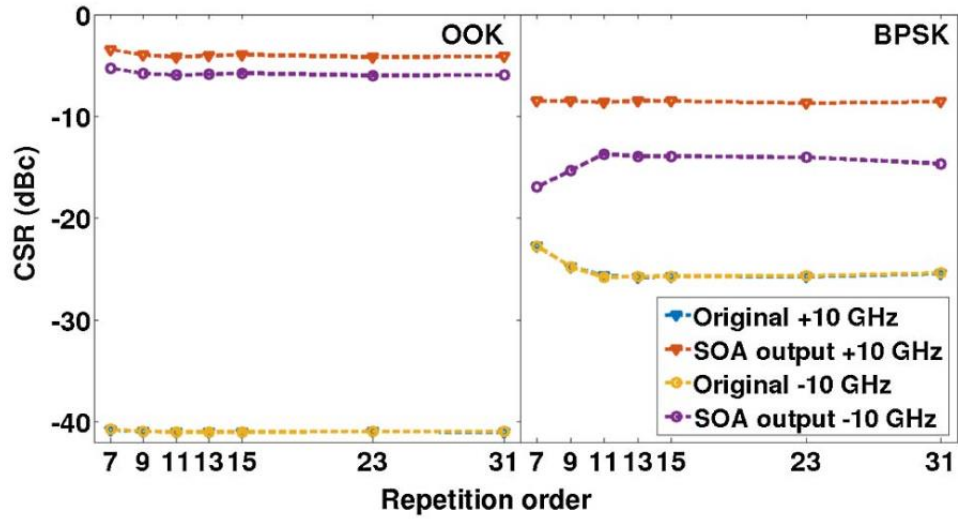
Fig. 7. Comparison of CSR of the 10 GHz and −10 GHz side-bands in the original and enriched signals with respect to PRBS order for NRZ-OOK (left) and NRZ-BPSK (right) formats.
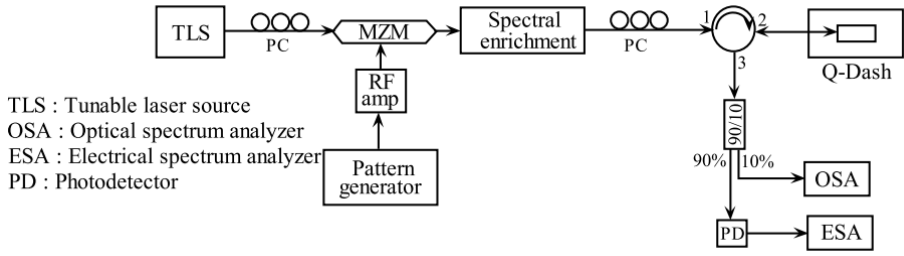
Fig. 8. Schematic diagram of the experimental setup employed for injection locking using enriched NRZ-OOK or NRZ-BPSK signal.
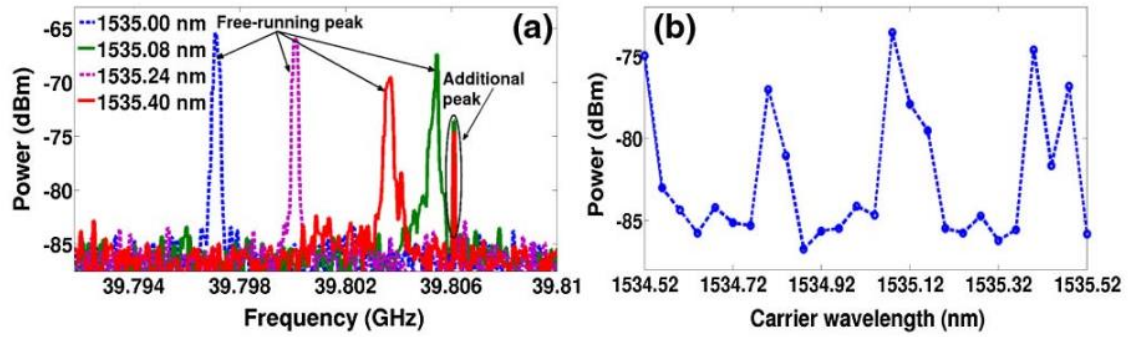
Fig. 9. (a) RF beat spectrum for injection of enriched data at 1535 nm carrier (span 20 MHz, RBW 10 kHz); (b) power at fourth harmonic of injected signal (39.806 GHz) for various values of carrier wavelength.
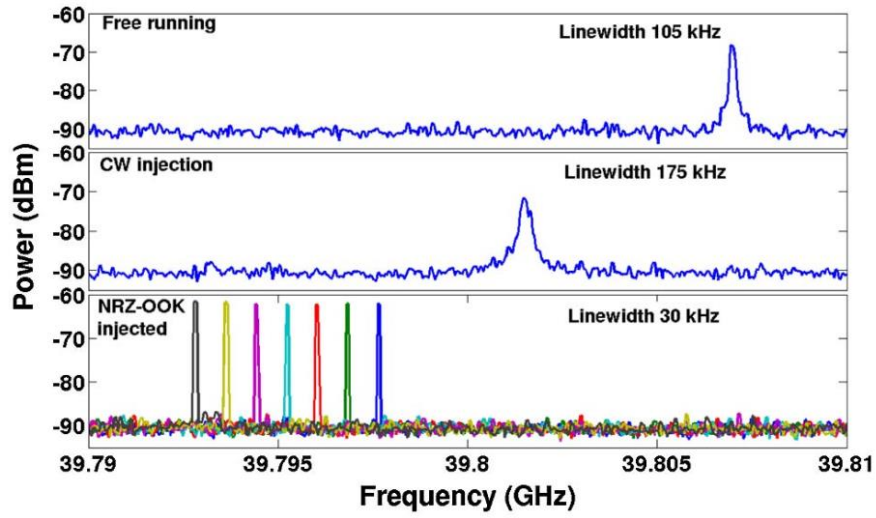
Fig. 10. RF beat spectrum of Q-dash laser output in free-running condition (top), with CW injection (middle), and with injection of spectrally enriched NRZ-OOK signal (bottom) for various values of data rate (span 20 MHz, RBW 3 kHz).
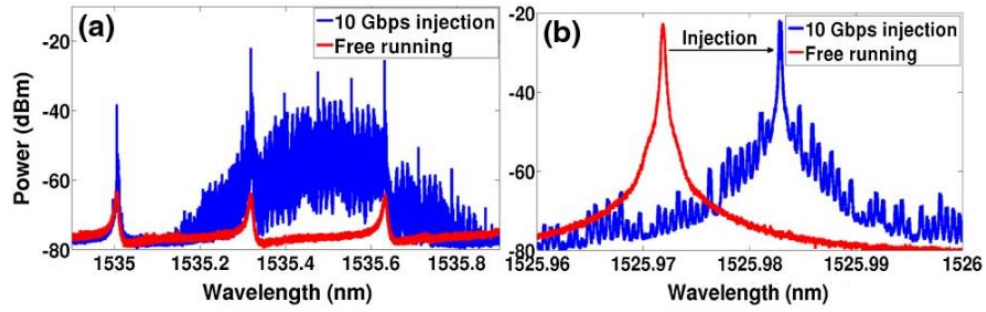
Fig. 11. (a) Optical spectrum upon injection of an enriched signal at 1535.40 nm (RBW 0.16 pm). (b) Optical spectrum of one mode of the Q-dash in the free-running condition and the injection-locked condition.
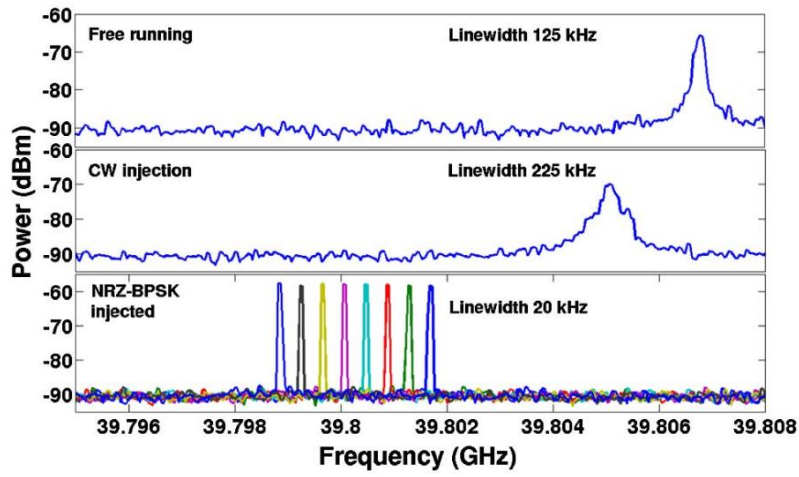
Fig. 12. RF beat spectrum of Q-dash laser output in free-running condition (top), with CW injection (middle), and with injection of spectrally enriched NRZ-BPSK signal (bottom) for various values of data rate (span 20 MHz, RBW 3 kHz).
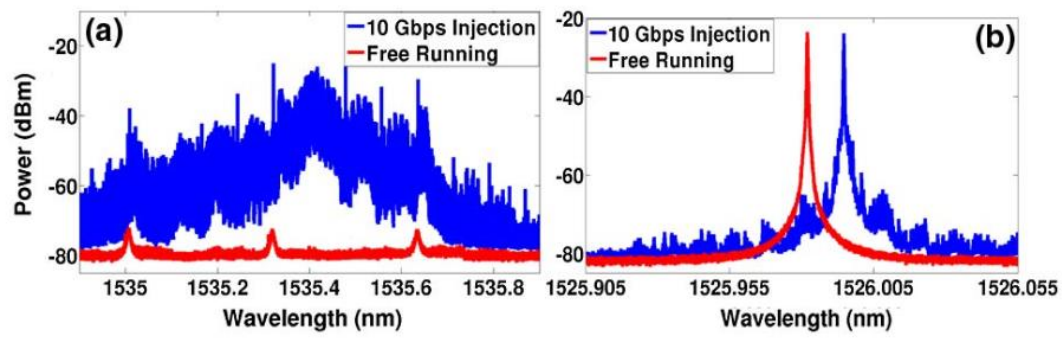
Fig. 13. (a) Optical spectrum upon injection of an enriched signal observed around the carrier wavelength. (b) Optical spectrum of one mode of the Q-dash in the free-running condition and the injection-locked condition.
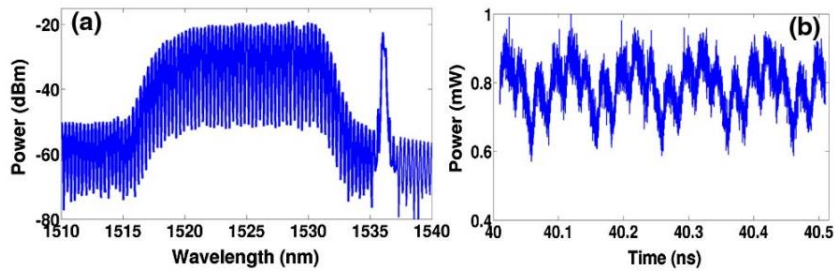
Fig. 14. (a) Optical spectrum and (b) time-domain trace of the out-put of the injection-locked Q-dash laser.
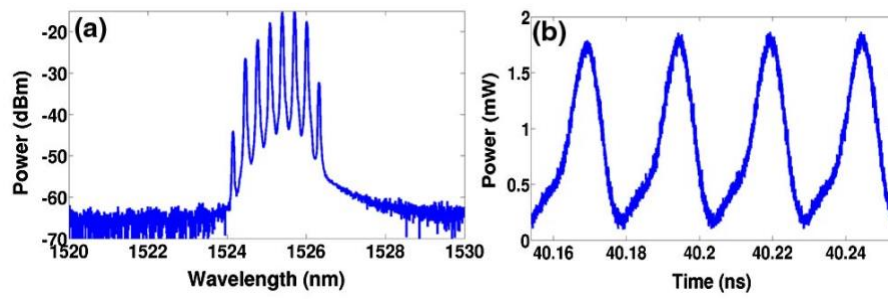
Fig. 15. (a) Filtered modes of Q-dash laser after injection locking; (b) 40 GHz signal obtained after filtering.

Table

Table 1. Comparison of Operating Conditions and Locking Range for Injection Locking with OOK and BPSK Data

Parameter	OOK	BPSK
Carrier wavelength	1535.4 nm	1535.4 nm
Q-dash bias current	190 mA	190 mA
Free-running frequency	39.807 GHz	39.8068 GHz
SOA bias current	200 mA	400 mA
Injected power	9.57 dBm	10.4 dBm
Baud rate	~9.95 Gbaud	~9.95 Gbaud
Locking range	5.2 MHz	2.8 MHz

24. M. Srivastava, P. M. Anandarajah, B. Srinivasan, S. O. Duill, D. Venkitesh, and P. Landais, "Sub-harmonic injection-locking of quan-tum dash laser through spectral enrichment for all-optical clock recov-ery," in Conference on Lasers and Electro-Optics (CLEO) (Optical Society of America, 2015), paper JTh2A.65.

25. N. C. Kothari and D. J. Blumenthal, "Influence of gain saturation, gain asymmetry, and pump/probe depletion on wavelength conversion efficiency of FWM in semiconductor optical amplifiers," IEEE J. Quantum Electron. 32, 1810–1816 (1996).

26. A. Bogatov, P. Eliseev, and B. Sverdlov, "Anomalous interaction of spectral modes in a semiconductor laser," IEEE J. Quantum Electron. 11, 510–515 (1975).

27. G. Agrawal and N. A. Olsson, "Self-phase modulation and spectral broadening of optical pulses in semiconductor laser amplifiers," IEEE J. Quantum Electron. 25, 2297–2306 (1989).

28. S. O. Duill and L. Barry, "Improved reduced models for single-pass and reflective semiconductor optical amplifiers," Opt. Commun. 334, 170–173 (2015).

29. K. Sato and H. Toba, "Reduction of mode partition noise by using semiconductor optical amplifiers," IEEE J. Sel. Top. Quantum Electron. 7, 328–333 (2001).